Parkinson's disease is a type of amyloidosis featuring accumulation of amyloid fibrils of α-synuclein

Katsuya Araki[a,b], Naoto Yagi[c,1], Koki Aoyama[c], Chi-Jing Choong[a], Hideki Hayakawa[a], Harutoshi Fujimura[d], Yoshitaka Nagai[e], Yuji Goto[f], and Hideki Mochizuki[a,1]

[a]Department of Neurology, Osaka University Graduate School of Medicine, Suita, 565-0871 Osaka, Japan; [b]Department of Neurology, Toyonaka Municipal Hospital, Toyonaka, 560-8565 Osaka, Japan; [c]Japan Synchrotron Radiation Research Institute (JASRI/SPring-8), Sayo, 679-5198 Hyogo, Japan; [d]Department of Neurology, Toneyama National Hospital, Toyonaka, 560-8522 Osaka, Japan; [e]Department of Neurotherapeutics, Osaka University Graduate School of Medicine, Suita, 565-0871 Osaka, Japan; and [f]Institute for Protein Research, Osaka University, Suita, 565-0871 Osaka, Japan

Edited by David S. Eisenberg, University of California, Los Angeles, CA, and approved July 25, 2019 (received for review April 16, 2019)

Many neurodegenerative diseases are characterized by the accumulation of abnormal protein aggregates in the brain. In Parkinson's disease (PD), α-synuclein (α-syn) forms such aggregates called Lewy bodies (LBs). Recently, it has been reported that aggregates of α-syn with a cross-β structure are capable of propagating within the brain in a prionlike manner. However, the presence of cross-β sheet-rich aggregates in LBs has not been experimentally demonstrated so far. Here, we examined LBs in thin sections of autopsy brains of patients with PD using microbeam X-ray diffraction (XRD) and found that some of them gave a diffraction pattern typical of a cross-β structure. This result confirms that LBs in the brain of PD patients contain amyloid fibrils with a cross-β structure and supports the validity of in vitro propagation experiments using artificially formed amyloid fibrils of α-syn. Notably, our finding supports the concept that PD is a type of amyloidosis, a disease featuring the accumulation of amyloid fibrils of α-syn.

Parkinson's disease | Lewy body | cross-β structure | X-ray diffraction

Senile plaques (SPs) of Alzheimer's disease (AD) are mainly composed of amyloid-β (Aβ) (1). Lewy bodies (LBs) of Parkinson's disease (PD) (2, 3) or dementia with LBs (2, 3) and glial cytoplasmic inclusions (GCIs) of multiple system atrophy (4) are mainly composed of α-syn. Recent work suggests that these aggregates can propagate from cell to cell, between interconnected brain regions, and even to recipient brains of different species (5–9). Isolated Aβ and α-syn proteins can aggregate in vitro in several days (10–12) to form amyloid fibrils with a cross-β structure (13). It has been shown that the fragments of these amyloid fibrils, so-called "seeds" or "preformed fibrils" of α-syn, when injected into the cells or the brains of mice, could propagate and be transmitted (8, 9). These phenomena are reminiscent of prion protein propagation. Protein structural conversion causes prion propagation. However, the structure of protein aggregates in patient brains is unknown. Although the seeds of α-syn may have propagated in the brains of mice (8, 9), there has been no direct evidence that the aggregates found in the brains of PD patients actually comprise a cross-β structure. Nonetheless, many studies and even clinical trials targeting the inhibition or elimination of α-syn aggregation have been performed based on such preconceptions. If amyloid seeds indeed propagate in the patient's brain, it is of great interest to structurally characterize the aggregates in the brain to see if they contain a cross-β structure.

There are excellent electron microscopic studies that have shown fibril-like structures in the aggregates (14–16). However, they are only morphological observations and do not provide information on the secondary structure of the proteins. Similarly, although Congo-Red staining is a useful technique for the detection of classical and/or pathological amyloids, its specificity for the cross-β structure is not high (17, 18).

One method to analyze the secondary or tertiary structure of proteins is Fourier-transform infrared (FTIR) spectroscopy (19, 20). Some FTIR studies showed that SPs are rich in β-sheets (21–23). We also reported that LBs have a β-sheet-rich structure (24). However, although FTIR is instrumental in analyzing the secondary structure of proteins, it does not directly indicate fibrillar organization of the structure.

To identify the characteristic periodic structure of the cross-β structure, XRD or electron diffraction is suitable. A cross-β diffraction pattern from amyloid fibrils consists primarily of a sharp reflection with a 0.47-nm spacing and a relatively broad reflection with an ∼1.0-nm spacing (25). However, there are very few XRD reports on in situ biological samples (26, 27).

In the present study, we performed microbeam XRD, a technique more specific for analyzing fibrillar structures, on LBs in thin sections of PD patients' brains to examine the presence of cross-β fibrils.

Results

Senile Plaques in Mouse Brains. To test the sensitivity of our microbeam XRD technique, SPs in mouse brains were scanned with an X-ray microbeam. The SPs in the brains of AD model mice (amyloid precursor protein [APP]/presenilin-1 [PS-1] knock-in mice) were identified with Congo-Red staining. Isolated plaques were selected by inspection with an optical microscope (Fig. 1*E*). Then, an area including a plaque was scanned with an X-ray microbeam of 6 μm in diameter. A 2D map of total wide-angle X-ray scattering intensity showed a distinct peak with a size corresponding to the plaque (Fig. 1*D*). Since X-ray scattering intensity generally depends on the amount of mass in the beam,

Significance

Lewy bodies (LBs), which mainly consist of α-syn, are neuropathological hallmarks of patients with Parkinson's disease (PD). Recently, it has been reported that aggregates of α-syn with cross-β structures are capable of propagating within the brain in a prionlike manner. However, there is still no evidence that such propagation occurs in the patient's brain. Here, we examined LBs in thin sections of autopsy brains of patients with PD using microbeam X-ray diffraction (XRD) and confirmed that aggregates of α-syn with a cross-β structure exist in brains of PD patients. Our finding supports the concept that PD is a type of amyloidosis, a disease featuring the accumulation and propagation of amyloid fibrils of α-syn.

Author contributions: K. Araki, N.Y., Y.N., Y.G., and H.M. designed research; K. Araki, N.Y., K. Aoyama, C.-J.C., H.H., and H.F. performed research; N.Y. contributed new reagents/analytic tools; K. Araki, N.Y., and Y.G. analyzed data; and K. Araki, N.Y., C.-J.C., Y.N., and H.M. wrote the paper.

The authors declare no conflict of interest.

This article is a PNAS Direct Submission.

[1]To whom correspondence may be addressed. Email: yagi@spring8.or.jp or hmochizuki@neurol.med.osaka-u.ac.jp.

This article contains supporting information online at www.pnas.org/lookup/suppl/doi:10.1073/pnas.1906124116/-/DCSupplemental.

Published online August 19, 2019.

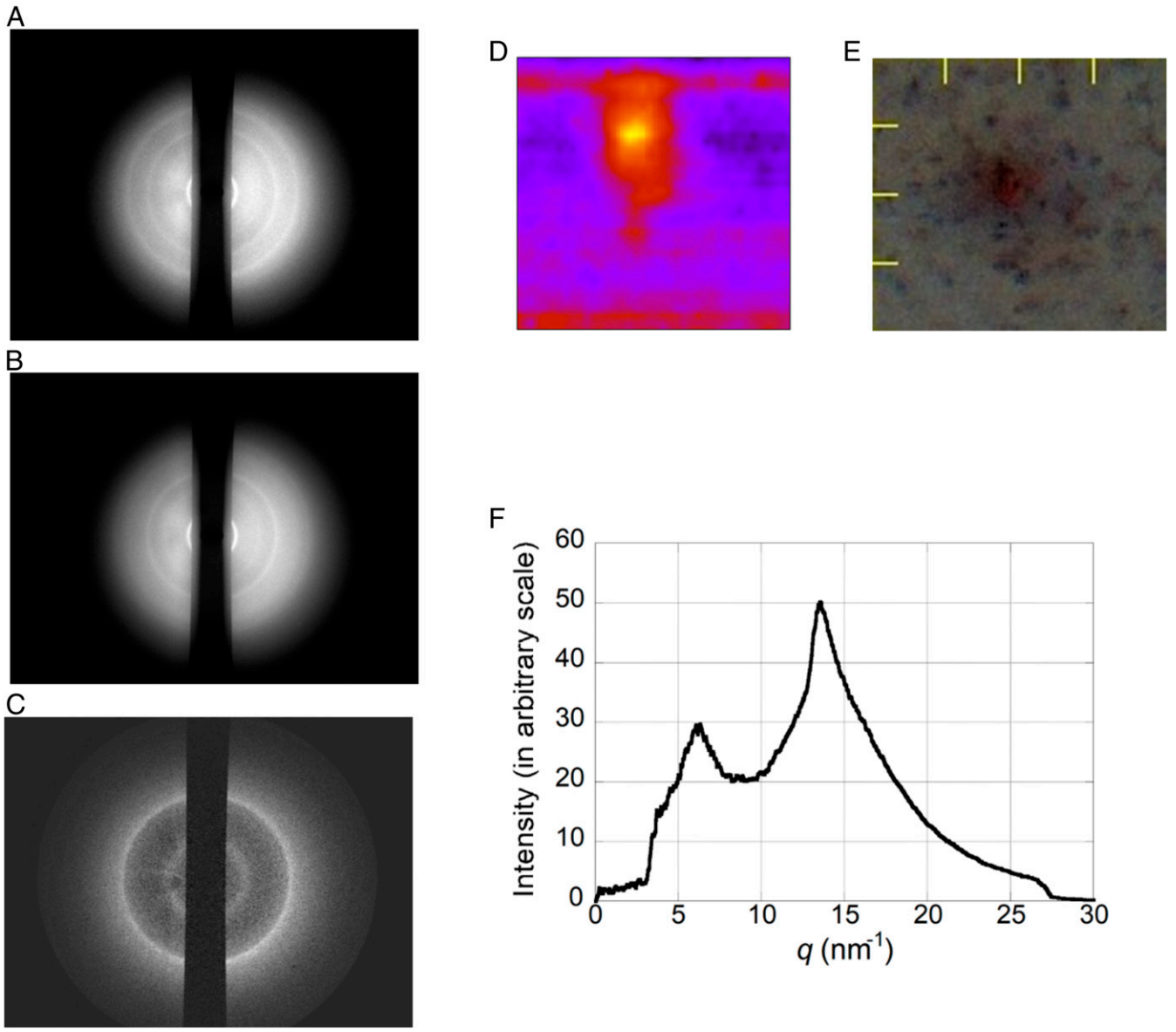

Fig. 1. Microbeam XRD analysis of mouse SPs showing a sharp diffraction peak corresponding to d = 0.47 nm. (*A*) "Top" image. (*B*) "Bottom" image. (*C*) Difference image obtained by subtracting *B* from *A*. (*D*) A 2D map of total wide-angle scattering intensity. A 40 × 40 scan was performed with 5-μm steps. (*E*) Optical micrograph of a Congo-Red–stained brain slice. Because the optical axis of the microscope was not perfectly coaxial with the X-ray beam, the areas in *D* and *E* are slightly misaligned. (Scale bar, 50 μm.) (*F*) Circularly averaged X-ray scattering intensity profile of *C*.

this peak is considered to correspond to the SP. A "difference" in X-ray scattering pattern obtained by subtracting the background pattern (Fig. 1*B*) from a high intensity pattern (Fig. 1*A*) showed 2 peaks at around q = 6.1 and 13.5 nm^{-1} ($q = 4\pi \sin\theta/\lambda$, where θ is half the scattering angle and λ is the wavelength of the X-rays), corresponding to Bragg spacings of d = 1.03 and 0.47 nm, respectively (Fig. 1 *C* and *F*), which are typically found in the diffraction pattern from synthetic amyloid fibrils (25). Particularly, the peak at q = 13.5 nm^{-1} is attributed to a β-sheet structure (25). Other plaques in the same section showed similar features in the X-ray intensity plots (*SI Appendix*, Figs. S1-1–S1-3). In some plaques, a peak was observed around q = 15 nm^{-1} (*SI Appendix*, Figs. S1-2 and S1-3), which may originate from lipids (28, 29).

LBs in Human Brains. Figs. 2–4 show the result for LBs from human brains. LBs were identified by staining with an antibody to α-syn (Fig. 2*E*). Isolated LBs were selected by inspection with the optical microscope (Fig. 2*E*). As was performed with SPs from mouse brains, a difference scattering pattern was obtained (Fig. 2*C*), and the peaks typical of amyloid fibrils at q = 6.1 and 13.5 nm^{-1} (d = 1.03 and 0.47 nm) were observed (Fig. 2 *C* and *F*) in some LBs. Another example of a similar result is shown in *SI Appendix*, Figs. S2-1 and S2-2. Such sharp peaks were observed 3 times out of 32 measurements. These were from the same patient (Pt. 1). In our previous study with synchrotron FTIR (24), the periphery of a LB tended to have higher β-sheet content than the center, which was rich in lipids. Although such a staining pattern was sometimes observed by optical microscopy (*SI Appendix*, Figs. S2-1*E* and S4-1*E*), the total X-ray scattering intensity of the region did not always show such a hollow distribution. Although the presence of lipids could be confirmed by the presence of a diffraction peak as in the mouse SP above, a clear lipid peak was not observed in the diffraction from human LBs.

In some other brain slices from the same or another patient (Fig. 3 and *SI Appendix*, Figs. S3-1 and S3-2), LBs were detected by antibody staining (Fig. 3*E*) and a marked peak in the 2D map

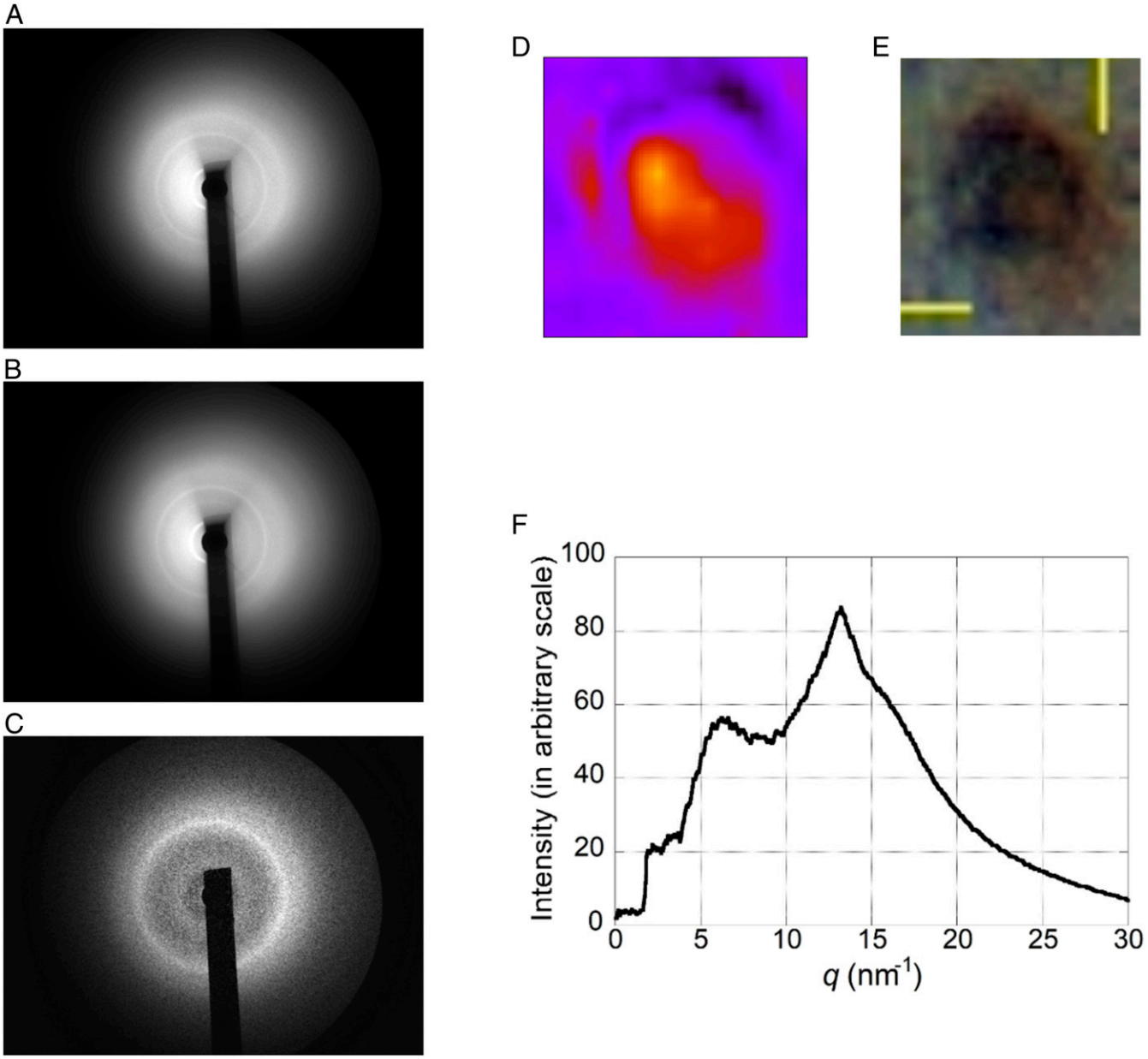

Fig. 2. Analysis of human LBs showing a sharp diffraction peak corresponding to d = 0.47 nm (sample from patient 1 [Pt. 1]). (*A*) Top image. (*B*) Bottom image. (*C*) Difference image obtained by subtracting *B* from *A*. (*D*) A 2D map of total wide-angle scattering intensity. A 20 × 20 scan was performed with 3-μm steps. (*E*) Micrograph of an antibody-stained brain section. (Scale bar, 10 μm.) (*F*) Circularly averaged X-ray scattering intensity profile of *C*.

of total scattering intensity was observed (Fig. 3*F*), but the peak at q = 13.5 nm^{-1} (d = 0.47 nm) was not as sharp as that in Fig. 2*E*. Slices from another patient (Fig. 4 and *SI Appendix*, Figs. S4-1 and S4-2) had a peak in the 2D scattering intensity map (Fig. 4*D*), but the scattering in the high intensity region in the map showed only a broad intensity peak in the region with a slightly larger spacing than that of typical amyloid peaks (Fig. 4 *C* and *F*). Thus, although strong immunostaining indicates the presence of high density of α-syn, the protein may not be forming amyloid fibrils in these cases. These results suggest the diversity of α-syn aggregates in the brains of PD patients.

To summarize, 1 brain slice from each of the 3 neuropathologically confirmed PD patients was analyzed by microbeam XRD. In the slice from Pt. 1, 21 antibody-stained LBs were scanned, and 20 of them showed isolated intensity peaks in the 2D map, 20 showed a broad intensity with q = 5–15 nm^{-1}, and 3 showed a sharp peak at q = 13.5 nm^{-1}, originating from the regular stacking of β-sheets. In patient 2 (Pt. 2), these numbers were 3, 2, 2, and 0, respectively, and in patient 3 (Pt. 3), the values were 8, 5, 3, and 0, respectively.

Even when the 1.03- and 0.47-nm diffraction peaks were observed from LBs, they were generally weaker than those from SPs in mouse brains. Congo-Red dye is reported to enhance the 0.47-nm peak of β-sheets in SPs (30), possibly by binding regularly to amyloid fibrils. The less marked 0.47-nm peak in LBs may partially result from the use of antibody staining. To eliminate the effects of the staining, we tried to measure the unstained samples. However, as we could not identify the aggregates in the unstained samples, we were unable to obtain data that could be analyzed.

Discussion

We first analyzed SPs in mouse brains by scanning with an X-ray microbeam and detected a peak characteristic for cross-β structures.

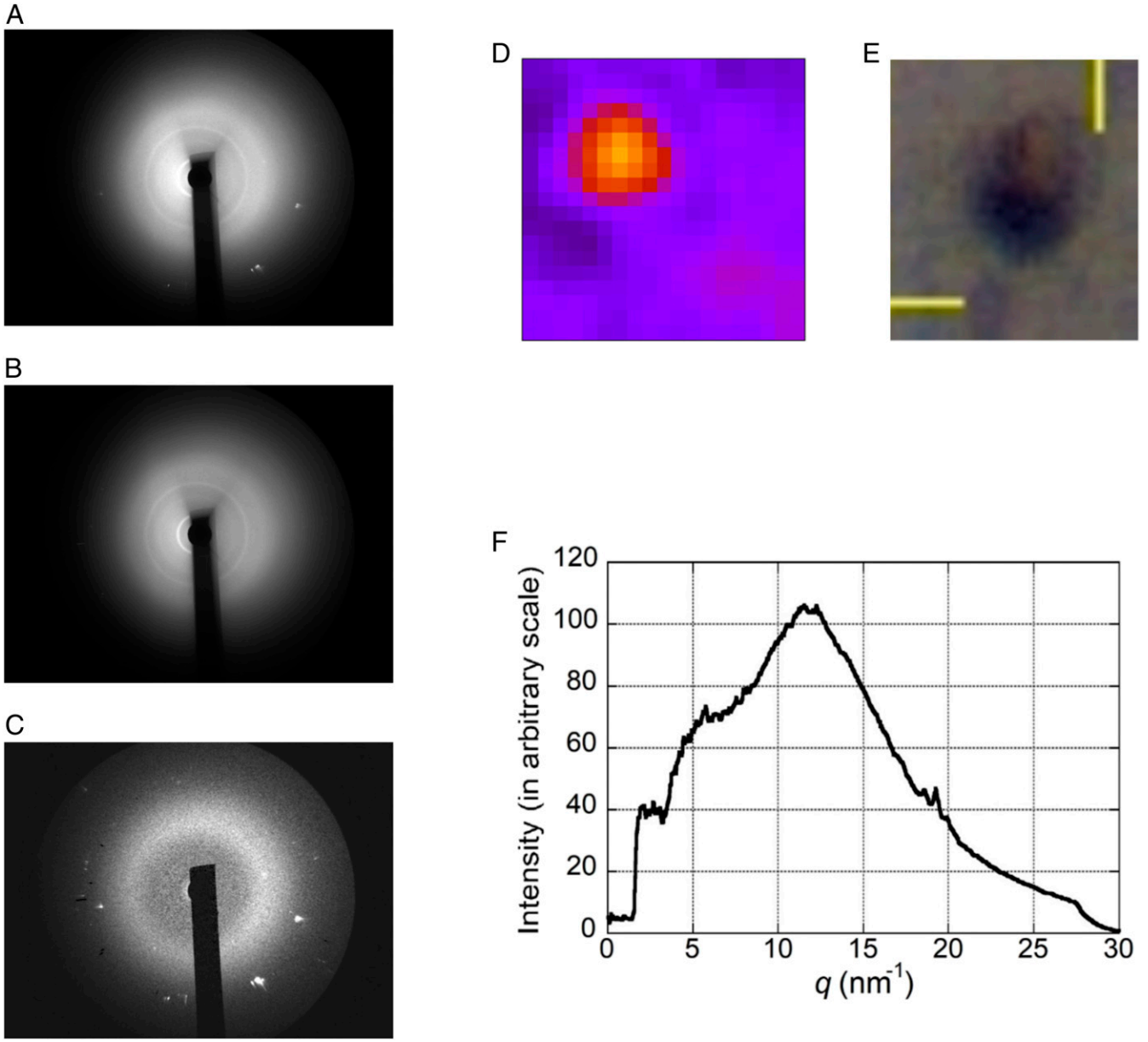

Fig. 3. Analysis of human LBs showing a broad peak around d = 0.47 nm. (*A*) Top image (sample from Pt. 1). (*B*) Bottom image. (*C*) Difference image obtained by subtracting *B* from *A*. (*D*) A 2D map of total wide-angle scattering intensity. A 20 × 20 scan was performed with 3-μm steps. (*E*) Micrograph of an antibody-stained brain section. (Scale bar, 10 μm.) (*F*) Circularly averaged X-ray scattering intensity profile of *C*.

Then, we tried to measure human SPs that were stained with an anti-Aβ antibody. However, we were unable to obtain data suitable for analysis because formic acid treatment was required for the immunostaining of human SPs with the anti-Aβ antibody. Such treatment was not required for the immunostaining of human LBs with an anti-α-syn antibody. Owing to the substantial changes caused by formic acid treatment, we were unable to simply compare aggregates stained by different methods.

The present study shows that some of the LBs in the brain of PD patients have a cross-β structure. The result supports the validity of propagation experiments using artificially formed amyloid fibrils of α-syn. However, typical amyloid peaks were not always observed in the X-ray scattering profile. It seems that LBs that are typically seen by immunostaining are not always rich in the cross-β structure. The results from the 3 patients show that many of the LBs identified by antibody staining are devoid of the ordered stacking of β-sheets. However, as shown in our previous synchrotron FTIR study (24), it is likely that these LBs also contain a high concentration of β-sheets. These results suggest that there is a variety in the state of amyloid proteins in the brain. There are several reasons for this variety. First, it may be due to different maturity stages of LBs. LBs at various stages of aggregation are expected to coexist in a brain. Second, it may be due to the heterogeneity of the fibril structure. A sharp 0.47-nm diffraction peak requires a large number of regularly spaced β-sheets. The stacking of β-sheets may be variable among different aggregates and may, hence, give rise to variation in peaks. Because there are many impurities in the brain, it is natural to think that α-syn does not form a uniform fibril structure as in in vitro experiments. These structural differences may cause symptomatic differences. Finally, variations due to technical problems, such as unevenness in section thickness, cannot be ruled out completely.

Clarification of the structural differences between LBs and Lewy neurites would be very interesting. However, to conclude

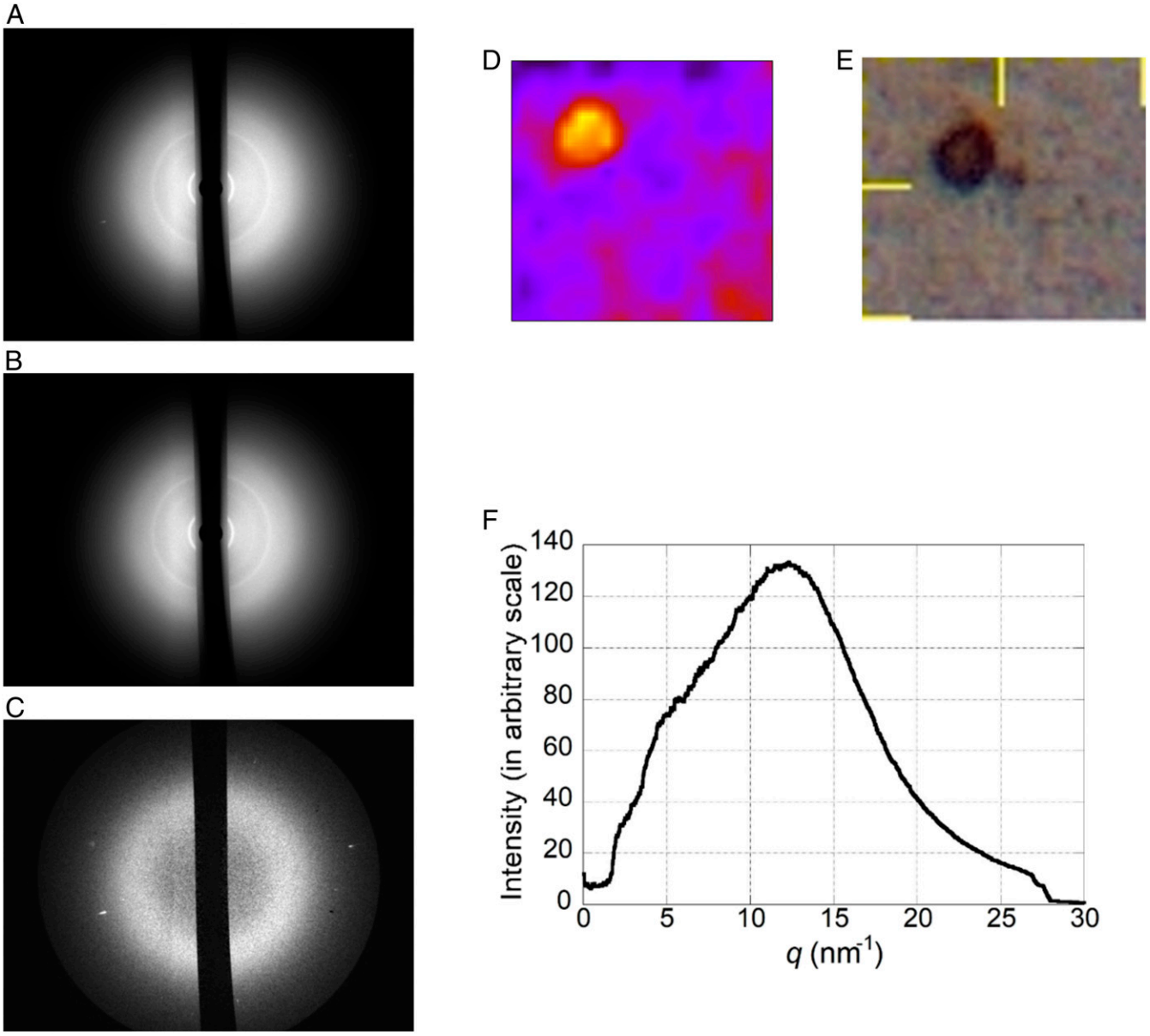

Fig. 4. Analysis of human LBs not showing a peak corresponding to d = 0.47 nm (sample from Pt. 2). (*A*) Top image. (*B*) Bottom image. (*C*) Difference image obtained by subtracting *B* from *A*. (*D*) A 2D map of total wide-angle scattering intensity. A 20 × 20 scan was performed with 5-μm steps. (*E*) Micrograph of an antibody-stained brain section. (Scale bar, 10 μm.) (*F*) Circularly averaged X-ray scattering intensity profile of *C*.

that a stained region is a Lewy neurite, it is necessary to make a section in a specific direction. We believe that the aggregate in *SI Appendix*, Fig. S4-4 is a Lewy neurite, but some of the other LBs analyzed in this study may also be neurites. At present, we do not have a reliable method to identify Lewy neurites in randomly cut sections. Therefore, in this study, we did not distinguish Lewy neurites and LBs but measured all aggregates stained with an anti-α-syn antibody.

Here, it should be noted that our similar measurements for GCIs have never shown sharp peaks (*SI Appendix*, Figs. S5-1–S5-3). Thus, GCIs may not contain amyloid fibrils. GCIs are found in glial cells, whereas LBs are present in neurons. In addition, it has been reported that GCIs are easier to propagate than LBs (6). It will be interesting to clarify the association between the ease of propagation and the structure of the aggregates. However, in this study, because the brain samples containing the GCIs were unfixed frozen samples, their results cannot be directly compared with the results of the LBs. In general, formalin-fixed frozen brain samples are rarely stored routinely. Although it will be difficult to obtain a sufficient number of such samples to perform statistical analyses, we would like to measure LBs and GCIs that were processed in the same way and report the differences between their structures with reliable accuracy in the near future.

On the other hand, the present paper shows that antibody staining does not always indicate a region rich in β-sheets. Even though stained regions gave strong scattering, showing that there are protein aggregates, they did not always give strong reflections from β-sheets. Immunostaining can indicate the localization of a protein of interest, but it cannot determine the conformation of a protein.

By classical histopathological definition, amyloid is a Congo-Red–stained extracellular proteinaceous deposit with a β-sheet structure (30). However, this definition has come into question when some amyloid species have been observed intracellularly and some, although demonstrably cross-β sheet, do not show Congo-Red positivity. Over the past decade, a more explicit and

uniform biophysical definition has been largely adopted in which amyloid fibrils are fibrillar polypeptide aggregates with cross-β conformations (17, 30). In our previous study with synchrotron FTIR (24), we found an abundance of β-sheets in LBs in PD patient brains. Since the requirement for sample preparation is different for FTIR and XRD, the same sample was not measured with the 2 techniques. FTIR identifies β-sheet structures by vibrational modes of atomic bonds, while XRD detects repeated structures of the β-sheet. In the present study, XRD confirmed that α-syn forms β-fibrils in human LBs. LBs, an intracellular deposit primarily composed of α-syn that is generally not stained with Congo Red, does not meet the criteria of classical amyloid but fits the recent biophysical definition well with its typical cross-β structure. PD is presently described as a heterogeneous multisystem neurodegenerative disease as α-syn deposits are not restricted to the central nervous system but are also found in the peripheral nerves innervating visceral organs, such as the heart and the gut (31). Supporting this concept, most PD patients experience a premotor period characterized by a variety of nonmotor symptoms that precede the onset of motor dysfunction. Given the multiple organ involvement of α-syn pathology, PD may be considered a systemic rather than a localized amyloidosis, featuring the accumulation of amyloid fibrils of α-syn.

Materials and Methods

All experimental protocols were approved by the Ethical Review Board at Osaka University Graduate School of Medicine and Toneyama National Hospital and were performed in accordance with the Ethical Guidelines for Clinical Research of the Ministry of Health, Labor and Welfare of Japan. Informed consent was previously obtained from all subjects.

Preparation of Mouse Brain Sections. Brain tissue samples from AD model mice APP/PS-1 knock-in mouse) (32, 33) were fixed in 4% buffered paraformaldehyde and frozen. Sections with 20-μm thickness were cut from the samples and deposited on Kapton polyimide films. Tissue sections were stained with Congo Red. Before measurements, these samples were dried at room temperature.

Preparation of Human Brain Sections. Brain tissue samples from 3 patients with neuropathologically confirmed PD were used for the measurements, i.e., a 75-y-old man (Pt. 1), a 76-y-old man (Pt. 2), and an 83-y-old woman (Pt. 3). All samples were of the midbrain. The brain samples were fixed in 4% buffered formaldehyde and frozen according to routine tissue processing for pathological examination. For each sample, 20-μm-thick sections were cut and deposited on Kapton polyimide films. Tissue sections from PD patient brains were incubated with the primary antibody, pSyn#64 (antihuman phosphorylated α-syn [Ser129] monoclonal antibody, Wako), followed by incubation with horseradish peroxidase-conjugated antimouse IgG (Dako EnVision+ System, Dako). Final staining was completed with incubation in 3,3′-diaminobenzidine + substrate chromogen for 5–10 min. Before measurements, these samples were dried at room temperature.

Microbeam XRD. Brain sections were scanned with a micro-X-ray beam at the BL40XU beamline in SPring-8 (Hyogo, Japan). An X-ray microbeam was obtained using a pinhole with a diameter of 5 μm (34). The sections were scanned in the X and Y directions with a step size of either 3 or 5 μm. Scans with 10, 20, or 40 steps in each direction were performed. At each point of the scan, a wide-angle X-ray scattering pattern was recorded. The X-ray wavelength was 0.083 nm with a bandwidth of about 2% (35). The X-ray detector was an X-ray image intensifier (V7739P, Hamamatsu Photonics, Hamamatsu, Japan) coupled with either a CCD camera (C4742-98–24ER 1344 × 2018 pixels) or a scientific complementary metal-oxide semiconductor camera (C11440-22CU. 2048 × 2018 pixels), both from Hamamatsu Photonics. Exposure time was 0.3–0.5 s. Sample-to-detector distance was about 115 mm. A vacuum path was not used.

X-ray Data Analysis. The basic assumption in the data analysis is that SPs or LBs, which comprise aggregated amyloid fibrils with high density, should produce stronger X-ray scatter than other regions of the brain. Thus, a map of total wide-angle scattering intensity was compared with a microscope image of the stained sections. For each scan, 100, 400, or 1,600 XRD patterns were obtained. Total scattering intensity in a diffraction pattern at each point was calculated, and a 2D intensity map was made. If the SPs or LBs identified by chemical staining contain a high density of amyloid fibrils, a high intensity region is expected to show up in the same area of the 2D intensity map.

Then, 5 points where the highest intensity was observed in the 2D map were searched. These are usually in the central part of the identified peak region. An averaged diffraction pattern of images obtained at these 5 points was treated as the top image (Fig. 1*A*). Similarly, diffraction patterns at half of the points that had lower intensity than the other half were averaged as the bottom image (Fig. 1*B*). The top image was considered to be recorded from the region with aggregates of amyloid fibrils, while the bottom image was considered to represent the background without protein accumulation. A difference image obtained by subtracting the bottom image from the top image (Fig. 1*C*) was regarded to represent diffraction from amyloid fibrils only. The strong rings seen in the top and bottom images are due to a Kapton sheet that was used to mount the brain section. These were completely removed by the subtraction.

ACKNOWLEDGMENTS. The authors are grateful to K. Namba (Graduate School of Frontier Biosciences, Osaka University) for suggesting the technique used in this paper. This work was performed with the approval of SPring-8 Program Review Committee (Grants 2013A1671, 2013B1737, 2014A1712, 2014B1811, 2015A1858, 2016B1235, 2017B1281, and 2018A1117). This work was supported by Japan Society for the Promotion of Science KAKENHI Grants JP18H02741 (to H.M.), JP16K09716 (to K. Araki), Ministry of Education, Culture, Sports, Science and Technology KAKENHI Grant JP17H06352 (to Y.G), JSPS Core-to-Core Program A (Advanced Research Networks) (to Y.N., Y.G., and H.M.), and Japan Agency for Medical Research and Development (AMED) Grants JP17hm0102037 (to Y.G. and H.M.) and JP19dm0207070 (to H.M.).

1. T. Iwatsubo *et al.*, Visualization of A β 42(43) and A β 40 in senile plaques with end-specific A β monoclonals: Evidence that an initially deposited species is A β 42(43). *Neuron* **13**, 45–53 (1994).
2. M. G. Spillantini, R. A. Crowther, R. Jakes, M. Hasegawa, M. Goedert, α-Synuclein in filamentous inclusions of Lewy bodies from Parkinson's disease and dementia with lewy bodies. *Proc. Natl. Acad. Sci. U.S.A.* **95**, 6469–6473 (1998).
3. M. Baba *et al.*, Aggregation of α-synuclein in Lewy bodies of sporadic Parkinson's disease and dementia with Lewy bodies. *Am. J. Pathol.* **152**, 879–884 (1998).
4. M. I. Papp, P. L. Lantos, The distribution of oligodendroglial inclusions in multiple system atrophy and its relevance to clinical symptomatology. *Brain* **117**, 235–243 (1994).
5. L. C. Walker, M. Jucker, Neurodegenerative diseases: Expanding the prion concept. *Annu. Rev. Neurosci.* **38**, 87–103 (2015).
6. S. B. Prusiner *et al.*, Evidence for α-synuclein prions causing multiple system atrophy in humans with parkinsonism. *Proc. Natl. Acad. Sci. U.S.A.* **112**, E5308–E5317 (2015).
7. A. Recasens *et al.*, Lewy body extracts from Parkinson disease brains trigger α-synuclein pathology and neurodegeneration in mice and monkeys. *Ann. Neurol.* **75**, 351–362 (2014).
8. K. C. Luk *et al.*, Pathological α-synuclein transmission initiates Parkinson-like neurodegeneration in nontransgenic mice. *Science* **338**, 949–953 (2012).
9. M. Masuda-Suzukake *et al.*, Prion-like spreading of pathological α-synuclein in brain. *Brain* **136**, 1128–1138 (2013).
10. C. Soto, Unfolding the role of protein misfolding in neurodegenerative diseases. *Nat. Rev. Neurosci.* **4**, 49–60 (2003).
11. K. A. Conway, J. D. Harper, P. T. Lansbury, Accelerated *in vitro* fibril formation by a mutant α-synuclein linked to early-onset Parkinson disease. *Nat. Med.* **4**, 1318–1320 (1998).
12. B. I. Giasson, K. Uryu, J. Q. Trojanowski, V. M. Lee, Mutant and wild type human α-synucleins assemble into elongated filaments with distinct morphologies *in vitro*. *J. Biol. Chem.* **274**, 7619–7622 (1999).
13. J. Greenwald, R. Riek, Biology of amyloid: Structure, function, and regulation. *Structure* **18**, 1244–1260 (2010).
14. J. X. Lu *et al.*, Molecular structure of β-amyloid fibrils in Alzheimer's disease brain tissue. *Cell* **154**, 1257–1268 (2013).
15. K. Arima *et al.*, Immunoelectron-microscopic demonstration of NACP/α-synuclein-epitopes on the filamentous component of Lewy bodies in Parkinson's disease and in dementia with Lewy bodies. *Brain Res.* **808**, 93–100 (1998).
16. H. Takahashi, K. Wakabayashi, The cellular pathology of Parkinson's disease. *Neuropathology* **21**, 315–322 (2001).
17. M. Fändrich, On the structural definition of amyloid fibrils and other polypeptide aggregates. *Cell. Mol. Life Sci.* **64**, 2066–2078 (2007).
18. R. Khurana, V. N. Uversky, L. Nielsen, A. L. Fink, Is Congo red an amyloid-specific dye? *J. Biol. Chem.* **276**, 22715–22721 (2001).
19. A. Barth, Infrared spectroscopy of proteins. *Biochim. Biophys. Acta* **1767**, 1073–1101 (2007).
20. G. Zandomeneghi, M. R. Krebs, M. G. McCammon, M. Fändrich, FTIR reveals structural differences between native β-sheet proteins and amyloid fibrils. *Protein Sci.* **13**, 3314–3321 (2004).

21. C. R. Liao *et al*., Synchrotron FTIR reveals lipid around and within amyloid plaques in transgenic mice and Alzheimer's disease brain. *Analyst* **138**, 3991–3997 (2013).
22. L. P. Choo *et al*., In situ characterization of beta-amyloid in Alzheimer's diseased tissue by synchrotron Fourier transform infrared microspectroscopy. *Biophys. J.* **71**, 1672–1679 (1996).
23. L. M. Miller *et al*., Synchrotron-based infrared and X-ray imaging shows focalized accumulation of Cu and Zn co-localized with beta-amyloid deposits in Alzheimer's disease. *J. Struct. Biol.* **155**, 30–37 (2006).
24. K. Araki *et al*., Synchrotron FTIR micro-spectroscopy for structural analysis of Lewy bodies in the brain of Parkinson's disease patients. *Sci. Rep.* **5**, 17625 (2015).
25. L. C. Serpell, J. Berriman, R. Jakes, M. Goedert, R. A. Crowther, Fiber diffraction of synthetic α-synuclein filaments shows amyloid-like cross-β conformation. *Proc. Natl. Acad. Sci. U.S.A.* **97**, 4897–4902 (2000).
26. F. Briki *et al*., Synchrotron x-ray microdiffraction reveals intrinsic structural features of amyloid deposits in situ. *Biophys. J.* **101**, 486–493 (2011).
27. J. Liu *et al*., Amyloid structure exhibits polymorphism on multiple length scales in human brain tissue. *Sci. Rep.* **6**, 33079 (2016).
28. M. De Felici *et al*., Structural characterization of the human cerebral myelin sheath by small angle x-ray scattering. *Phys. Med. Biol.* **53**, 5675–5688 (2008).
29. N. Yagi, A scanning SAXS/WAXS study of rat brain. *J. Phys. Conf. Ser.* **272**, 012009 (2011).
30. J. D. Sipe *et al*., Nomenclature 2014: Amyloid fibril proteins and clinical classification of the amyloidosis. *Amyloid* **21**, 221–224 (2014).
31. E. Gelpi *et al*., Multiple organ involvement by alpha-synuclein pathology in Lewy body disorders. *Mov. Disord.* **29**, 1010–1018 (2014).
32. K. Lok *et al*., Characterization of the APP/PS1 mouse model of Alzheimer's disease in senescence accelerated background. *Neurosci. Lett.* **557**, 84–89 (2013).
33. S. Takeda *et al*., Diabetes-accelerated memory dysfunction via cerebrovascular inflammation and Abeta deposition in an Alzheimer mouse model with diabetes. *Proc. Natl. Acad. Sci. U.S.A.* **107**, 7036–7041 (2010).
34. N. Ohta *et al*., Structural analysis of cell membrane complex of a hair fibre by microbeam X-ray diffraction. *J. Appl. Cryst.* **38**, 274–279 (2005).
35. K. Inoue *et al*., Present status of high flux beamline (BL40XU) at SPring-8. *Nucl. Instrum. Methods Phys. Res. Sect. A* 467–468, 674–677 (2001).